

Structure and thermal history dependant phase behavior of hydrated
synthetic sphingomyelin analogue:
1,2-dimyristamido-1,2-deoxyphosphatidylcholine

Hiroshi Takahashi^{1*}, Yukihsa Okumura², and Junzo Sunamoto³

- 1) Department of Physics, Gunma University, Maebashi, 371-8510, Japan
- 2) Department of Chemistry and Material Engineering, Shinshu University, Nagano, 380-8553, Japan
- 3) Professor Emeritus, Kyoto University, Kyoto, Japan

*Corresponding author,

Department of Physics, Gunma University, 4-2 Aramaki, Maebashi, 371-8510, Japan
Tel&Fax +81-27-220-7552, E-mail address: htakahas@fs.aramaki.gunma-u.ac.jp

Regular paper/Biomembrane

Keywords:

acylamino-phospholipid; phase behavior; metastability; hydrogen bond;
differential scanning calorimetry; X-ray diffraction

(Accepted April 30 2005 BBA)

Summary

The physical properties of hydrated multilamellar sample of 1,2-dimyristamido-1,2-deoxyphosphatidylcholine (DDPC) were investigated by means of differential scanning calorimetry (DSC), static X-ray diffraction, and simultaneous DSC and X-ray diffraction. The DDPC is a synthetic sphingomyelin analogue and has two amide bonds in its hydrophobic parts. This paper reports on metastable phase behavior of the hydrated DDPC sample. By cooling from a chain-melted state at the rates of greater than $4\text{ }^{\circ}\text{C min}^{-1}$, hydrated DDPC bilayers form a metastable gel phase. In the gel phase, the hydrophobic chains are tilted with respect to the bilayer normal, as like the gel phase of glycerophosphatidylcholines. By heating, the metastable gel phase is transformed into a stable phase associated with an exothermic heat event at $18.3\text{ }^{\circ}\text{C}$ ($\Delta H = 14.6\text{ kJ mol}^{-1}$) and then the stable phase is transformed into a liquid-crystalline phase at $25.6\text{ }^{\circ}\text{C}$ ($\Delta H = 42\text{ kJ mol}^{-1}$). The incubation at $17\text{ }^{\circ}\text{C}$ for more than 1 hour also induces the formation of the stable phase. In the stable phase, the hydrophobic chains are packed into highly ordered crystal-like structure. However, the X-ray diffraction pattern of the stable phase suggested that the entire DDPC molecules do not form a two-dimensional molecular ordered lattice, differing from normal subgel phase of glycerophosphatidylcholines. The structure and phase behavior of DDPC revealed by the present study are discussed from the viewpoint of hydrogen bonds.

1. Introduction

Acylamino-phospholipid, 1,2-dimyristamido-1,2-deoxyphosphatidylcholine (DDPC) has two amide bonds, instead of two ester bonds in dimyristoylphosphatidylcholine (DMPC) (Fig.1). The DDPC was synthesized as an analogue of sphingomyelin by Sunamoto et al. [1]. One of their motivations was to create an artificial boundary lipid. Jost et al. [2] first proposed the concept of boundary lipid, based on their electron spin resonance (ESR) study of the interaction between phospholipids and cytochrome oxidase. The boundary lipid is defined as the layer of lipids surrounding an integral membrane protein in which the mobility of the lipids is restricted in comparison with that of bulk lipids. From 1970s to early 1990s, it was speculated that sphingomyelin is one of candidates of the boundary lipid in biomembranes, because it was suggested that sphingomyelin's amide group can bind to an integral membrane protein by forming a hydrogen bond [3]. Based on such a situation, Sunamoto et al. designed the chemical structure of DDPC [1]. Nuclear magnetic resonance (NMR) study has revealed that DDPC interacts with glycoporphin strongly in comparison with DMPC, indicating that DDPC behaves as boundary lipid-like for glycoporphin in DDPC/DMPC mixed bilayers [4]. This conclusion has been also supported by ESR study [5]. Furthermore, it has been revealed that addition of DDPC to a liposome enhance the efficiency of protein transfer from various biological systems to the liposome [6-11].

In spite of considerable effort, there is no direct evidence that sphingomyelin acts as boundary lipid in natural biomembranes. However, a renewed interest in sphingomyelin has emerged from the late 1990s, in connection with the concept of functional lipid domains, so-called "lipid rafts" [12-14]. The lipid rafts are constituted of cholesterol and sphingolipids (sphingomyelin and glycosphingolipids, such a like, GM1-ganglioside) and incorporate specific proteins such as glycosylphosphatidylinositol (GPI)-anchored proteins, doubly acylated proteins, palmitoylated transmembrane proteins, etc. The lipid domains are thought to play important roles in many biological processes, such as, signaling, membrane fusion, lipid

sorting, and protein trafficking. Recently, it has been suggested that the hydrogen bond between the amide group of the sphingolipid ceramide backbone and the 3'-OH group of cholesterol is one of key factors for the formation of lipid rafts [15,16]. In addition, Masserini and Ravasi [17] have proposed a hypothesis that an intermolecular hydrogen bond between hydroxyl and amide groups of the ceramide moiety of sphingolipids is also one of the main driving forces of lipid raft formation.

Hence, it is of interest to study the physical properties of lipids having amide bonds, such as DDPC. This work aims to get basic knowledge on the physical properties that is needed to discuss the function of the lipids having amide bonds in the lipid rafts and the molecular mechanism of DDPC-enhanced protein transfer.

After the succession of DDPC synthesis, studies on the physical properties of DDPC have been carried out with the use of various techniques [1,4,18-20]. In these previous studies, no structural investigation has been performed. The detailed phase behavior depending on thermal history has not been examined, although the appearance of metastable phases has been reported for many natural and synthetic sphingomyelin bilayer systems [21-23]. In the present study, we investigated the thermal and structural properties of the DDPC bilayers, paying attention to the thermal history dependant phase behavior. For this purpose, in addition to normal differential scanning calorimetry (DSC) and static X-ray diffraction, simultaneous DSC and X-ray diffraction measurements were performed with the use of a synchrotron radiation X-ray beam. Here, we report that after rapid cooling from a chain-melted state, DDPC forms a metastable gel phase and that the gel phase is transformed into a stable crystal-like phase with an exothermic process by heating scan.

2. Materials and methods

2.1 Materials

Acylamino-phospholipid, 1,2-dimyristamido-1,2-deoxyphosphatidylcholine (DDPC), was synthesized from a starting material, diaminopropanol. The detailed

methods of the synthesis and purification have been reported elsewhere [1]. Dipalmitoyl-*L*- α -phosphatidylcholine (DPPC) and poly(vinylpyrrolidone) (PVP) of average molecular weight 40,000 were purchased from Sigma (St. Louis, MO). The DPPC had a purity >99% and were used without further purification. Water used in this study was prepared with a Mill-Q system (Millipore Corp., Bedford, USA).

2.2 Sample preparation

For DSC, hydrated samples were prepared directly in DSC sample pans. Amounts of 1 to 2 mg of the dry lipid samples were accurately weighed and sealed in aluminum DSC sample pans with 15 mg of pure water. The lipid concentrations were about 7-14 wt%. To get homogeneity, heating and cooling scans from 0 °C to 60 °C were performed repeatedly until that identical DSC curves were obtained.

For simultaneous X-ray diffraction and calorimetry and static X-ray diffraction, to get sufficient X-ray diffraction intensity and heat flow, relatively high concentrated samples were prepared as below. About 20 mg of dry lipid samples were weighed and then put into an Eppendorf tube with 0.5 ml pure water. The lipid and water were heated up about 70 °C and kept for 5 min. Then, the samples were agitated on a vortex mixer at a room temperature. These cycles of heating and agitating were repeated at least five times. Next, to concentrate the samples in the Eppendorf tube were centrifuged with a temperature-controlled centrifuge (MX-150, Tomy Ltd., Tokyo, Japan) with 15,000 rpm for about 60 min at 40 °C. After the centrifugation, supernatant water was removed. Judging from the weight, the lipid concentrations of the samples treated with this procedure were about 30-40 wt%.

2.3 Differential scanning calorimetry

DSC measurements were performed with a DSC6100-Exstra6000 thermal analysis system (Seiko Instruments Inc., Chiba, Japan). The scan rate was usually 1.0 or 2.0 °C min⁻¹. Data acquisition and analysis were carried out using software provided by Seiko Instruments Inc. High-purity gallium and indium were used to calibrate the DSC signals.

2.4 Static X-ray diffraction

Static X-ray diffraction patterns were recorded using a two-dimensional area detector (Imaging plate, Fuji Photo Film Co. Ltd., Tokyo, Japan) and a rotating anode X-ray generator (RU200BEH, Rigaku, Tokyo, Japan) operating at 50 kV and 30 mA. The X-ray beam was focused by a double-mirror optical system and Cu K α radiation ($\lambda = 0.1542$ nm) was selected using a Ni filter. The sample was sealed in a fine wall quartz capillary with 1.5 mm diameter. The capillary was fixed to a brass hollow holder. Temperature of the sample was controlled by circulating water from a temperature-controlled water bath to the sample mount. Typical exposure time was 4 hours. Several static X-ray diffraction patterns of DPPC bilayers were recorded using an X-ray scattering spectrometer installed at BL40B2 of 8 GeV synchrotron radiation source of Japan Synchrotron Radiation Research Institute (JASRI). The details of the spectrometer have been described elsewhere [24]. In the BL40B2, two-dimensional X-ray diffraction patterns were recorded with a Rigaku R-AXIS IV imaging plate system. The X-ray wavelength and the exposure time were 0.100 nm and 30 sec, repetitively. Two-dimensional diffraction data recorded on imaging plates were transformed into one-dimensional data by radial integration. This data conversion was performed using FIT2D software written by Dr. A. Hammersley (<http://www.esrf.fr/computing/scientific/FIT2D/>). The lattice spacings (d) and reciprocal spacing (S),

$$S = \frac{1}{d} = \frac{2 \sin \theta}{\lambda},$$

where 2θ is the scattering angle and λ is the wavelength of X-ray, were calibrated by the diffraction pattern of silver behenate powder crystals [25].

2.5 Simultaneous X-ray diffraction and differential scanning calorimetry

Simultaneous measurements with synchrotron radiation were performed at the station BL9C of Photon Factory at the High energy Accelerator Research Organization (KEK), Tsukuba, Japan. At the station, the focusing and monochromatizing of the

radiation X-ray beam were carried out using a bent mirror and a double Si(111) crystal monochromator. Further beam collimation was performed by means of three independent slit systems. The wavelength of X-ray used was 0.15 nm. By locating two position sensitive proportional one-dimensional counters at different positions, both small-angle and wide-angle diffraction data were recorded simultaneously. In addition, thermal data were collected simultaneously with the use of a modified differential scanning calorimeter that was originally developed for use in optical microscopy. Details of the modification of the calorimeter, the set-up and the sample cell used have been described elsewhere [26]. The DSC data were recorded for the temperature range from 0 °C to 40 °C with the scan rate of 2.0 °C/min, but, the exposure of X-ray beam was limited to the temperature range from 5 °C to 35 °C. Thus, total exposure time was about 20 min. For the present set up, the beam intensity at sample position was less than about 10^{10} photons/sec. This intensity is relatively weak in comparison with that of other synchrotron small angle scattering stations equipped with an insertion device, such as variable gap wiggler or undulator. However, because the exposure time is comparatively long, it is necessary to evaluate the degree of radiation damage carefully. Judging from the following facts, we concluded that there is no serious radiation damage of the sample. It has been reported that radiation damage induces a change of lipid phase transition temperature and a disordering of lamellar stacking [27, 28]. In the present study, such like phenomena were not observed. After finish of the simultaneous measurement, we recorded again X-ray diffraction pattern at 5 °C of the sample used the measurement. The diffraction pattern almost agrees with that of the fresh sample subjected to the same thermal history. The widths and relative intensities of each diffraction peak were the same within error for both samples.

2.6 Calculation of electron density profiles

One-dimensional electron density profiles across the bilayer, $\rho(x)$, on a relative electron density scale were calculated from

$$\rho(x) = \frac{F(0)}{L} + \frac{2}{L} \sum_{h=1}^{h=h_{\max}} \{\exp(i\alpha(h))\} F(h) \cos\left(\frac{2\pi x h}{L}\right),$$

where L is the lamellar spacing, $F(h)$ is the structure amplitude, x is the distance from the center of the bilayer, and $\alpha(h)$ is the phase angle for each lamellar diffraction order h . The value of $\exp\{i\alpha(h)\}$ should be +1 or -1, because lipid bilayers are expected to a centersymmetric system. Before converting structure amplitudes from diffraction intensities, the observed lamellar diffraction intensities of each peak were corrected for the Lorenz and polarization factors and normalized according to standard methods [29]. The determination of the phase angle, $\alpha(h)$, was achieved using so-called swelling method. In the method, it is assumed that the structure of lipid bilayer hardly depends on the change of hydration level, i.e., the change of water layer thickness. On the basis of this assumption, the structure amplitude curve of the bilayers is traced experimentally by varying the thickness of water layers. Only finite number of data can be obtained experimentally. Thus, in order to trace continuous structure amplitude curve, the Shannon sampling theorem was used according to the proposal by Sayre [30]. To vary the thickness of the water layers between the DDPC bilayers, an osmotic stress was applied to the hydrated samples. For the chain melted state samples, an osmotic stress by neutral water-soluble polymer (poly(vinylpyrrolidone)) was applied [31,32], and for other cases, an osmotic stress by ice was applied [33]. The mechanism of generating an osmotic stress is described briefly as follows. Poly(vinylpyrrolidone) molecules cannot exist at water layers between lipid bilayers, because the average molecular weight of the polymer used in this study is relatively high (40,000) and the thickness of the water layers is relatively small ($< \sim 1$ nm). Owing to this size problem, ice crystals also tend to grow in the water region of outside of multilamellar phospholipid vesicles. Because the polymer and ice crystals cannot penetrate lipid bilayers, these materials existing outside of the vesicles give an osmotic stress and reduce the thickness of water layers between lipid bilayers. The Shannon sampling theorem was also used to estimate the value of $F(0)$, according to proposal by King and Worthington [34] as follows. Assuming $F(0) = 0$, we first determined the phase angle set by tracing continuous structure amplitude curve as described above. Afterwards, the value of $F(0)$ was estimated for all data to fit the best by the sampling theorem. It has been pointed out that another method for estimating the $F(0)$ value using

the data of volume measurement is superior to this method from a viewpoint of accuracy [35,36]. However, the advantage of the method we used is that one can estimate the $F(0)$ value only from lamellar X-ray diffraction data. In this paper, we will discuss mainly the peak positions of electron density profiles. The peak positions do not depend on the $F(0)$ value, if the phase angle estimation is correct. This is a reason why we used this method.

3. Results

3.1 Differential scanning calorimetry

We found that the phase behavior of hydrated DDPC bilayers depends on the thermal history. Figure 2 shows typical DSC thermograms recorded with a scan rate of $1.0\text{ }^{\circ}\text{C min}^{-1}$. The thermogram A in Fig. 2 was obtained when the heating scan was begun immediately after cooling from $40\text{ }^{\circ}\text{C}$ to $0\text{ }^{\circ}\text{C}$ with a cooling rate of more than $-4.0\text{ }^{\circ}\text{C min}^{-1}$. The thermogram B in Fig. 2 was obtained for samples subjected to an incubating at $17\text{ }^{\circ}\text{C}$ for more than 1 hour before cooling to $0\text{ }^{\circ}\text{C}$. The DSC thermogram of the sample without incubation at $17\text{ }^{\circ}\text{C}$ (Fig. 2A) has three transition peaks, two endothermic and one exothermic. The smaller endothermic transition occurs at $16.5\text{ }^{\circ}\text{C}$ with a transition enthalpy of $1.7 \pm 0.2\text{ kJ mol}^{-1}$. Here, the endothermic direction is taken to be positive for the sign of the transition enthalpies. At just above the smaller endothermic peak, an exothermic peak is observed. The peak temperature is $18.3\text{ }^{\circ}\text{C}$ and the transition enthalpy is $-14.6 \pm 2.3\text{ kJ mol}^{-1}$. The bigger endothermic transition peak is observed at $25.6\text{ }^{\circ}\text{C}$ with a transition enthalpy of $42 \pm 1\text{ kJ mol}^{-1}$ for both samples with and without the incubating at $17\text{ }^{\circ}\text{C}$.

3.2 Static X-ray diffraction

The above DSC results suggest that there are three different phases. To identify the three phases, X-ray diffraction experiment was carried out. Figure 3 presents static X-ray diffraction patterns for hydrated DDPC samples recorded at $3.5\text{ }^{\circ}\text{C}$, $20\text{ }^{\circ}\text{C}$, and 30

°C. All samples were heated up to about 40 °C and cooled down to each measurement temperature. Before the measurements, samples were kept at each measurement temperature, at least 1 hour.

At 3.5 °C and 20 °C, several sharp diffraction peaks are observed in the small-angle regions with the ratio 1:1/2:1/3:1/4,..., indicating that the lipid molecules are organized in a stacked lamellar array. The lamellar spacings are 6.17 nm (3.5 °C) and 5.76 nm (20 °C). At 3.5 °C, a sharp diffraction peak is observed at $1/0.447 \text{ nm}^{-1}$ together with a relatively broad diffraction peak centered at $1/0.402 \text{ nm}^{-1}$, in the wide-angle region. Here, we call this phase by the term of lamellar gel phase or gel phase, simply. Similar diffraction patterns have been reported for a lamellar gel phase (or gel-like phase) with tilted chains of phosphatidylcholines or phosphatidylethanolamines at relatively low temperatures (near 0 °C and subzero temperatures) [37-39]. The authors of [38, 39] used the term "sub-subgel phase (SGII phase)" or "metastable ordered phase (L_{R1} phase)" to call the phase and discussed the existence of another phase transition between these phases and a normal lamellar gel phase.

At 20 °C, in addition to two main peaks at $1/0.431 \text{ nm}^{-1}$ and $1/0.407 \text{ nm}^{-1}$, small additional diffraction peaks are observed in the wide-angle region ($1/0.476 \text{ nm}^{-1}$, $1/0.431 \text{ nm}^{-1}$, $1/0.431 \text{ nm}^{-1}$ etc.). This pattern indicates that the hydrophobic chains are packed into a crystal-like highly ordered lattice. In this paper, we call this phase "highly ordered gel phase". By incubating at low temperatures for long time, hydrated glycerophosphatidylcholines forms an ordered phase [40-43], for which a term "subgel phase" is usually used. Later, we will discuss the difference between the highly ordered gel phase of DDPC and the subgel phase of glycerophosphatidylcholines.

At 30 °C, only two diffraction peaks are observed in the small-angle region. However, we concluded that a stacked lamellar array is also formed at 30 °C, judging from the ratio of two reflections is 1:1/2 and the fact that, by applying of osmotic pressure to the sample, we could detect higher order lamellar diffraction peaks as describe later. The lamellar spacing is 6.52 nm. The broad scattering profile in the wide-angle region indicates that the hydrophobic chains are melted state. Hence, the

phase at 30 °C is a lamellar liquid-crystalline phase.

3.3 Simultaneous X-ray diffraction and calorimetry

In order to investigate the relation between structural changes and thermal phase transition behavior, we carried out simultaneous X-ray diffraction and calorimetry measurements. Figure 4 displays the results obtained by the simultaneous measurements for the samples subjected to different thermal history treatments. The heating scan rate was 2.0 °C min⁻¹. In the DSC thermograms of the figure, to compare between X-ray diffraction and DSC data, by contrast to the usual way, the vertical axis is temperature and the horizontal axis is heat flow. From the results obtained by simultaneous measurements and the static X-ray diffraction patterns described above, it can be concluded that the phase sequences of hydrated DDPC samples are as following. (1) For the sample without incubating at 17 °C, after rapid cooling, the gel phase is formed and then, by heating, the gel phase is transformed into the highly ordered gel phase associated with endothermic and exothermic heat events in the temperature range from ~16 °C to ~20 °C. Finally, the highly ordered gel phase is transformed into the liquid-crystalline phase at ~26 °C. (2) The incubating at 17 °C for more than 1 hour induces the formation of the highly ordered gel phase. This highly ordered gel phase is converted directly into the liquid-crystalline phase at ~26 °C, by heating. In other word, the present results demonstrate that the gel phase of DDPC is a metastable phase.

3.4 Electron density profiles

In order to clarify the further detailed structures of each phase of the hydrated DDPC bilayers, electron density profiles have been reconstructed from the lamellae diffraction intensity data. Figure 5 displays the graphs in which, for three different temperatures, the normalized structure amplitude data are plotted as a function of reciprocal space S and the continuous transform curves are drawn using the Shannon sampling theorem. From these graphs, the phase sequence was deduced to be $-$, $-$, $+$, $-$ for all cases, and electron density profiles calculated using this phase set are shown in Fig. 6. In the present study, to vary the thickness of water layers, an osmotic stress by

neutral polymer (PVP) was applied to the hydrated DDPC sample at 30 °C. In the sample at 30 °C, although, for the sample in pure water, only two small angle diffraction peaks were observed, four diffraction peaks with a ratio of 1/1 : 1/2 : 1/3 : 1/4 were observed for the samples in polymer solution containing more than 30 wt% PVP, i.e., under high osmotic pressure conditions. For zero or low osmotic pressure conditions, it can be considered that, due to thermal fluctuation, the intensity of higher order lamellar diffraction peaks are too weak to detect experimentally. The calculated electron density profiles show typical characteristic features of "bilayer" structure (Fig. 6). In the electron density profiles, the two peaks in the profiles correspond to the electron-rich phosphate moieties of the polar head group of DDPC and the peak-to-peak distance (d_{p-p}) is one of the measures of the bilayer thickness. The values are written in the figure.

4. Discussion

The present study revealed that the hydrated DDPC forms three different phases: the stable highly ordered gel, metastable gel, and liquid-crystalline phases, and that the phase transition sequence depends on the thermal history. In addition, the present X-ray diffraction study characterized the structural properties of each phase. In order to address the feature of the amide bond of DDPC, we discuss the present results by comparing with literature data of sphingomyelins and glycerophosphatidylcholines.

The fatty acyl residue of natural sphingomyelins is a mixture of several species. Owing to this heterogeneity, it is difficult to interpret the experimental data on the physical properties of natural sphingomyelins. Hence, here we compare with data of synthetic chemically pure sphingomyelins. To our knowledge, however, there is no detailed report of the physical properties of synthetic chemically pure myristoylsphingomyelin that has hydrophobic chain lengths corresponding to DDPC. Thus, we compare our results with the reported results of synthetic pure stearoylsphingomyelin that is one of the most extensively studied sphingomyelins with two equivalent length hydrophobic chains. Bruzik and Tsai [22] have reported that

totally synthetic stereochemically pure *D-erythro* steraloysphingomyelin exhibits complex phase behavior depending on thermal history and that the lipid has three different gel phases: two are metastable and one is stable. This behavior is similar to that of DDPC, that is, both lipids have several different gel phases. NMR study [23] has revealed that the rotation of the phosphocholine headgroup of the *D-erythro* stearoysphingomyelin is frozen in the stable gel phase. From this viewpoint, the stable gel phase of the *D-erythro* stearoysphingomyelin is the same as the subgel phase of glycerophosphatidylcholines [43]. Later, we will discuss the problem of the headgroup rotation of DDPC in the highly ordered gel phase.

The synthetic method used in the present study produces racemic DDPC samples. On the basis of the results obtained by DSC, fluorescence spectroscopy, and X-ray diffraction, it has been revealed that *DL-erythro* steraloysphingomyelin also exhibits thermal history dependent phase behavior, that is, the *DL-erythro* stearoysphingomyelin has, at least, two gel phases: one is a metastable phase and the other is a stable phase [21]. The stable gel phase melts at 57 °C and gives rise to a number of sharp diffraction peaks in its wide angle X-ray diffraction pattern. The latter fact indicates that the packing of hydrophobic chains of the stable gel phase is more ordered than that typical phospholipid gel phase. This chain packing state is the same as that of the highly ordered gel phase of DDPC. In addition, under a certain thermal history condition, by heating, the metastable gel phase of *DL-erythro* stearoysphingomyelin is transformed into the stable phase after endothermic and one or more exothermic events (Fig.1B of the paper by Estep et al. [21]). Hence, except for the transition temperatures, the phase behavior of *DL-erythro* stearoysphingomyelin is very similar to that of DDPC revealed by the present study. Since detailed X-ray analyses have not been performed, we cannot continue any further comparative discussion on the structures of DDPC and the chemically pure synthetic sphingomyelins.

Next, let us compare the structures of DDPC in each phase with those of corresponding glycerophosphatidylcholine, i.e., dimyristoylphosphatidylcholine (DMPC). We recorded the static X-ray diffraction pattern of the liquid-crystalline

phase of DDPC at 30 °C and could detect only two lamellar diffraction peaks. Petracche et al. [44] have reported X-ray diffraction data of the liquid-crystalline phase of fully hydrated DMPC under various osmotic pressure conditions at the same temperature (30 °C). Although Petracche et al. [44] did not describe directly, judging from the Fig.4 of their paper, it seems that they could also observe only two orders of lamellar diffraction under no osmotic pressure condition. This is due to the thermal undulation of the fluid liquid-crystalline phase lipid bilayers. Under relatively high osmotic pressure conditions, Petracche et al. [44] have detected four orders of lamellar diffraction. From the electron density files calculated using the four orders, they have reported the d_{p-p} value of the liquid-crystalline phase of DMPC under 27 atm osmotic pressure to be 3.52 nm. In the present study, the d_{p-p} value of DDPC under 31 atm osmotic pressure is 3.60 nm (Fig. 6A). Both values are almost identical, taking account of the resolution of the electron density profiles calculated from only four orders of diffraction. This suggests that the bilayer structures are similar to both DMPC and DDPC in the liquid-crystalline phase.

For the gel phase of fully hydrated DMPC bilayers, Tristram-Nagle et al. [45] have estimated the d_{p-p} value of DMPC to be 4.01 ± 0.01 nm from high resolution electron density profile calculated using ten orders of lamellar diffraction obtained from the oriented sample. This value is almost identical with the d_{p-p} value of DDPC estimated here (4.03 nm), suggesting that the structures of DMPC and DDPC bilayers are almost the same in the gel phase. The hydrocarbon chains of DMPC are tilted to the bilayer normal in the gel phase [35-37, 45]. Hence, one can conclude that the hydrophobic chains of DDPC are tilted to the bilayer normal in the gel phase. This is also supported by the shape of wide-angle X-ray diffraction profile (Fig. 3A). The d_{p-p} value of the highly ordered gel phase of DDPC is almost same as that of the gel phase, indicating that the chains are also tilted in the highly ordered gel phase.

Subsequently, let us discuss the thermodynamic data. From the transition enthalpy values obtained by DSC, one cannot estimate absolute enthalpy values of each phase, but one can calculate the difference between any two phases. The difference enthalpy between the gel and liquid-crystalline phases of DDPC is calculated to be 29.1

kJ mol^{-1} ($= 42 - 14.8 + 1.7$). For DMPC, the value is calculated to be about 29 kJ mol^{-1} , using the literature values [37,46]. Those two values are almost identical. This supports the conclusion of the X-ray diffraction, i.e., the structures of DMPC and DDPC bilayers are almost the same in both gel and liquid-crystalline phases.

Finally, we discuss the highly ordered gel phase by comparing with the subgel phase of DMPC. The gel phase of DMPC bilayers is transformed into the subgel phase by incubating at low temperatures for long time. Lewis et al. [46] has reported that the gel phase of DMPC is also a metastable phase. The transition temperature from the stable subgel phase to a ripple phase of DMPC is about $2 \text{ }^\circ\text{C}$ higher than that from the metastable gel phase to the ripple phase, i.e., by heating, the subgel phase of DMPC bilayers converts directly into the ripple phase not the gel phase [46]. Interestingly, it has been recently revealed that myristoylpalmitoylphosphatidylcholine exhibits almost the same phase transition sequence [47].

In comparison with the difference enthalpy value between the liquid-crystalline and subgel phase of DMPC (50.7 kJ mol^{-1}) [46], the corresponding value between the liquid-crystalline and highly ordered gel phase of DDPC is apparently small (42 kJ mol^{-1}). This implies that the highly ordered gel phase of DDPC is less ordered than the subgel phase of DMPC. The subgel phases of glycerophosphatidylcholines are relatively dehydrated structures characterized by strongly interacting and fairly immobilized polar headgroups [41-43, 46, 48]. Furthermore, in the subgel phase, the entire lipid molecules form a two-dimensional ordered lattice [49] that gives rise to several X-ray diffraction peaks in middle-angle region ($S = 1.0 - 2.0 \text{ nm}^{-1}$) [41-43,47,49]. Figure 7 shows the middle- and wide-angle diffraction patterns of the highly ordered gel phase of DDPC and the subgel phases of dipalmitoylphosphatidylcholine (DPPC). It should be that the highly ordered gel phase of DDPC is compared with the subgel phases of DMPC. However, a complicated temperature treatment is necessary to achieve a formation of the subgel phase of DMPC [46]. While the formation of subgel phase of DPPC is relatively easily formed by only incubating at $0-4 \text{ }^\circ\text{C}$ for several days [40-43,48]. Strictly speaking, as revealed by detailed kinetic studies [50, 51], the incubation at $0-4 \text{ }^\circ\text{C}$ for several days cannot induce a complete homogenous subgel

phase formation for DPPC. The incubation causes that only 70-80% of the whole DPPC molecules convert into the subgel phase from the gel phase. However, the small remainder of gel phase does not greatly contribute to the X-ray diffraction profiles. Thus, here we use DPPC as the second best material to discuss the feature of highly ordered gel phase of DDPC. The diffraction peaks reflected from the two-dimensional molecular lattice, that are associated with ordering of the entire molecule including the headgroup, as well as of the hydrocarbon chains, are clearly observed for the subgel phase of DPPC. On the other hand, for the highly ordered gel phase of DDPC, no diffraction peak appears in the middle angle region except for higher order lamellar diffraction peaks. This indicates that the entire DDPC molecules in the highly ordered gel phase do not form an ordered two-dimensional lattice and that the molecular packing structure is relatively disordered as compared with that of the subgel phase of glycerophosphatidylcholines.

As mentioned above, although the structural features of DDPC bilayers are similar to that of glycerophosphatidylcholine bilayers for the gel and liquid-crystalline phases from various viewpoints, the structural features of highly ordered gel phase of DDPC differs from that of the subgel phase of glycerophosphatidylcholine. In the following, we will consider the origin that causes this difference from the viewpoint of the interaction around the amide bonds of DDPC bilayers. In addition, we will discuss the relation between the interaction around the amide bonds and the peculiar phase behavior of DDPC bilayers, i.e., the metastable gel phase is quickly transformed into the stable highly ordered gel phase by only heating.

It is believed that three different interactions mainly contribute to the formation of the subgel phase of glycerophosphatidylcholines: van der Waal interaction between hydrocarbon chains, polar interaction at the headgroups, and the interaction at the polar/apolar interfacial regions of lipid bilayers [46]. As pointed out by McElhaney and co-workers [46,48], because it is incompatible to maximize the three above-mentioned interactions in the bilayer structures, the optimization of three different interactions should be required to form the subgel phase of glycerophosphatidylcholines. On the other hand, the present X-ray diffraction study shows no ordering of headgroups of

DDPC in the highly ordered gel phase, suggesting that polar interaction at the headgroups does not mainly contribute to formation of the highly ordered gel phase. Hence, it can be presumed that the optimization of only two different interactions at the chain and polar/apolar interfacial regions of is required for the formation of the highly ordered gel phase of DDPC. This would be one of the reasons for the quick formation of the highly ordered gel phase of DDPC from the metastable gel phase by only heating. In addition, the hydrogen bonds formed at the amide groups of DDPC would contribute to the quick formation of the highly ordered gel phase.

Previous Fourier transform infrared and NMR spectroscopic studies [1,18] have indicated that the amide group of DDPC is linked through hydrogen bonding to a water molecule or to an adjacent hydrogen-accepting group. Hence, it is strongly suggested that an intermolecular lateral hydrogen bond network is formed between NH and CO groups, such like a network of hydrogen bonds proposed by Masserini and Ravasi [17], in order to explain the mechanism maintaining sphingolipid molecules correlated with each other in sphingolipid domains. It is very likely that, by this hydrogen bond network, the hydrophobic chain parts of DDPC tend to approach closely each other and to form easily a crystal-like ordered structure. The other hydrogen-accepting group of DDPC is the phosphate of the headgroup. On the basis of ^{31}P - NMR data, Zhou et al. [20] have suggested the formation of intramolecular hydrogen bonding between the amide and phosphate groups. Such the intramolecular hydrogen bonding has been reported for sphingomyelins [3, 52-54]. In addition, recent molecular dynamic simulation study [54] has shown that the hydrogen bond between the amide and phosphate group does not greatly inhibit the conformational freedom of the polar headgroup of sphingomyelin. It is expected that such same situation occurs for DDPC bilayers and that, a hydrogen-bonded phosphate-water network that is observed for DMPC crystal [55] is not formed in the stable highly ordered gel phase of DDPC. In conclusion, we infer that this nature of the intramolecular hydrogen bond of DDPC is one of the reasons for the fact that the DDPC headgroups do not form an ordered lattice while the hydrophobic chains are packed into a crystal-like structure in the stable highly ordered gel phase.

Acknowledgements

We thank Prof. M. Nomura and Mr. A. Koyama (Photon Factory, KEK) for their effort in the improvement of the optical system of the beamline 9C at the Photon Factory, Dr. K. Inoue (JASRI) for his help in measurements at the SPring8, and Prof. P.J. Quinn (King's College London) for his critical reading and comments on early version of this manuscript. The synchrotron X-ray measurements were performed under approval of the Photon Factory Program Advisory Committee (Proposal No. 2003G138) and the Program Advisory Committee of the Japan Synchrotron Radiation Research Institute (Proposal No. 2003A0354-NL2-np).

Figure Captions

Figure 1

Chemical structure of 1,2-dimyristamido-1,2-deoxyphosphatidylcholine (DDPC).

Figure 2

DSC thermograms of hydrated DDPC samples recorded at heating rate of $1.0\text{ }^{\circ}\text{C min}^{-1}$. (A) Heating scan after cooling from $40\text{ }^{\circ}\text{C}$ to $0\text{ }^{\circ}\text{C}$. (B) Heating scan after cooling from $17\text{ }^{\circ}\text{C}$ to $0\text{ }^{\circ}\text{C}$ following more than 1hr incubation at $17\text{ }^{\circ}\text{C}$.

Figure 3

Static X-ray diffraction patterns of hydrated DDPC samples recorded at (A) $3.5\text{ }^{\circ}\text{C}$, (B) $20\text{ }^{\circ}\text{C}$, and (C) $30\text{ }^{\circ}\text{C}$. Each inset shows the patterns of the wide-angle region.

Figure 4

Comparison among small- and wide-angle X-ray diffraction and DSC data obtained simultaneously for hydrated DDPC samples. The scanning rate was $2.0\text{ }^{\circ}\text{C min}^{-1}$. (A) Heating scan after cooling from $40\text{ }^{\circ}\text{C}$ to $0\text{ }^{\circ}\text{C}$. (B) Heating scan after cooling from $17\text{ }^{\circ}\text{C}$ to $0\text{ }^{\circ}\text{C}$ following more than 1hr incubation at $17\text{ }^{\circ}\text{C}$. For the DSC data, the horizontal and vertical axes represent heat flow and temperature, respectively.

Figure 5

Structure amplitudes and phase assignments of a hydrated DDPC sample at different temperatures: (A) $3.5\text{ }^{\circ}\text{C}$, (B) $20\text{ }^{\circ}\text{C}$, and (C) $30\text{ }^{\circ}\text{C}$. The solid curves are drawn using the Shannon sampling theorem.

Figure 6

Relative electron density profiles of a hydrated DDPC sample at different temperatures: (A) $3.5\text{ }^{\circ}\text{C}$, (B) $20\text{ }^{\circ}\text{C}$, and (C) $30\text{ }^{\circ}\text{C}$. For $30\text{ }^{\circ}\text{C}$, the DDPC samples were dispersed into

solution containing 30wt% PVP, i.e., under 6.8 atm osmotic pressure.

Figure 7

X-ray diffraction patterns of the subgel phase of hydrated (A) dipalmitoylphosphatidylcholine (DPPC) and (B) DDPC samples recorded at 20 °C. Before the measurement, the DPPC sample was kept at about 4 °C for one week to form the subgel phase. For DDPC, the pattern is the same as Fig.3B. To show relatively weak diffraction peaks clearly, the diffraction intensities are presented by logarithmic scale. The arrows indicate the diffraction peaks come from a two-dimensional ordered lattice formed by entire DDPC molecules. The marks, $d/5$, $d/6$,..., indicate that the peaks correspond higher order of lamellar diffraction.

Reference

- [1] J. Sunamoto, M. Goto, K. Iwamoto, H. Kondo, T. Sato, Synthesis and characterization of 1,2-dimyristoylamido-1,2-deoxyphosphatidylcholine as an artificial boundary lipid, *Biochim. Biophys Acta* 1024 (1990) 209-219.
- [2] P.C. Jost, O. H. Griffith, R. A. Capaldi, G. Vanderkooi, Evidence for boundary lipid in membranes, *Proc. Nat. Acad. Sci. USA* 70 (1973) 480-484.
- [3] C. F. Schmit, Y. Barenholz, T.E. Thompson, A nuclear magnetic resonance study of sphingomyelin in bilayer systems, *Biochemistry* 16 (1977) 2649-2656.
- [4] J. Sunamoto, K. Nagai, M. Goto, B. Lindoman, Deuterium nuclear magnetic resonance studies on the interaction of glycoprotein with 1,2-dimyristoylamido-1,2-deoxyphosphatidylcholine, *Biochim. Biophys. Acta* 1024 (1990) 220-226.
- [5] M. Goto, J. Sunamoto, Effect of artificial boundary lipid on the membrane dynamics of human glycoprotein-containing liposome, *Bull. Chem. Soc. Jpn.* 65 (1992) 3331-3334.
- [6] J. Sunamoto, M. Goto, K. Akiyoshi, Effective transfer of membrane proteins from human erythrocytes to artificial boundary lipid-containing liposomes, *Chem. Lett.* (1990) 1249-1252.
- [7] J. Sunamoto, K. Akiyoshi, M. Goto, T. Noguchi, T. Sato, E. Nakayama, R. Shibata, H. Shiku, Effective transfer of membrane proteins from intact cells to human liposomes and preparation of liposomal vaccines. *Ann. N. Y. Acad. Sci.* 613 (1990) 116-127.
- [8] Y. Okumura, M. Ishitobi, M. Sobel, K. Akiyoshi, J. Sunamoto, Transfer of

membrane proteins from human platelets to liposomal fraction by interaction with liposomes containing an artificial boundary lipid. *Biochim. Biophys. Acta* 1194 (1994) 335-340.

[9] M. Nakamura, Y. Katura, K. Tsujii, K. Kurihara, J. Sunamoto, Taste receptor proteins directly extracted by liposome from intact epithelium of bullfrog tongue, *Biochem. Biophys. Res. Commun.* 201 (1994) 415-422.

[10] M. Nakamura, K. Tsujii, J. Sunamoto, Liposome-induced release of cell membrane proteins from intact tissue epithelium, *Med. Biol. Eng. Comput.* 36 (1998) 645-653.

[11] K. Suzuki, Y. Okumura, T. Sato, J. Sunamoto, Membrane protein transfer from human erythrocyte ghosts to liposomes containing an artificial boundary lipid, *Proc. Japan Acad.* 71(B) (1995) 93-97.

[12] K. Simons, E. Ikonen, Functional rafts in cell, *Nature* 387 (1997) 569-572.

[13] D.A. Brown, E. London, Structure and origin of ordered lipid domains in biological membranes, *J. Membr. Biol.* 164 (1998) 103-114.

[14] A. Rietveld, K. Simons, The differential miscibility of lipids as the basis for the formation functional membrane rafts, *Biochim. Biophys. Acta* 1376 (1998) 467-479.

[15] Simons, K. Ikonen, E. 2000. How cell handle cholesterol, *Science* 290, 1721-1726.

[16] H. Ohva-Rekilä, B. Ramstedt, P. Leppimäki, J. P. Slotte, Cholesterol interaction with phospholipids in membranes, *Progr. Lipid Res.* 41 (2002)66-94-7.

[17] M. Masserini, D. Ravasi, Role of sphingolipids in the biogenesis of membrane domains, *Biochim. Biophys. Acta* 1532 (2001) 149-161.

- [18] T. Kawai, J. Umemura, T. Takenaka, M. Gotou, J. Sunamoto, Fourier transform infrared study on the phase transitions of a 1,2-bis(myristoylamido)-1,2-deoxyphosphatidylcholine-water system, *Langmuir* 4 (1988) 449-452.
- [19] D.W. Grainger, J. Sunamoto, K. Akiyoshi, M. Goto, K. Knutson, Mixed monolayers and cast films of acyl ester and acylamino phospholipids, *Langmuir* 8 (1992) 2479-2485
- [20] Z. Zhou, Y. Okumura, J. Sunamoto, NMR study of choline methyl group of phospholipids, *Proc. Japan Acad.* 72(B) (1996) 23-27.
- [21] T. N. Estep, W.I. Calhoun, Y. Barenholz, R.L. Biltonen, G.G. Shipley, T.E. Thompson, Evidence for metastability in stearyl sphingomyelin bilayers, *Biochemistry* 19 (1980) 20-24.
- [22] K.S. Bruzik, M.-D. Tasi, A calorimetric study of the thermotropic behavior of pure sphingomyelin diastereomers, *Biochemistry* 26 (1987) 5364-5368.
- [23] K.S. Bruzik, B. Sobon, G. M. Salamonyk, Nuclear magnetic resonance study of sphingomyelin bilayers, *Biochemistry* 29 (1990) 4017-4021.
- [24] K. Miura, M. Kawamoto, K. Inoue, M. Yamamoto, T. Kumasaka, M. Sugiura, A. Yamano, H. Moroyama, Commissioning for wide-angle routine proteomix beam line BL-40B2: Protein crystallography and small-angle scattering, *SPring-8 User Experiment Report* 4 (2000)168.
- [25] T. N. Blanton, T.C. Huang, H. Toraya, C.R. Hubbard, S.B. Robie, D. Louer, H.E. Gobel, G. Will, R. Gilles, T. Raftery, JCPDS-international center for diffraction data

round robin study of silver behenate, Powder Diffraction 10 (1995) 91-95.

[26] H. Takahashi, S. Matuoka, Y. Amemiya, I. Hatta, Simultaneous differential scanning calorimetry and time-resolved X-ray diffraction of lipid-water system I. Relationship between chain melting and endothermic heat at the main transition of a dipalmitoylphosphatidylcholine-water system, Chem. Phys. Lipids 76 (1995) 115-121.

[27] A. C. Cheng, J. L. Hogan, M. Caffrey, X-ray destroy the lamellar structure of model membranes. J. Mol. Biol. 229 (1993) 291-294.

[28] V. Cherezov, K. M. Riedl, M. Caffrey, Too hot to handle? Synchrotron X-ray damage of lipid membranes and mesophases. J. Synchrotron. Radiat. 9 (2002) 333-341.

[29] C. R. Worthington, A. E. Blaurock, A structure analysis of nerve myelin. Biophys. J. 9 (1969) 970-990.

[30] D. Sayre, Some implications of a theorem due to Shannon, Acta Crystallogr. Sect. B 5 (1952) 843.

[31] T. J. McIntosh, S. A. Simon, Hydration force and bilayer deformation: A reevaluation, Biochemistry 25 (1986) 4058-4066.

[32] X. Wang, H. Takahashi, I. Hatta, P. J. Quinn, An X-ray diffraction study of the effect of α -tocopherol in the structure and phase behavior of bilayers of dimyristoylphosphatidylethanolamine, Biochim. Biophys. Acta 1418 (1999) 335-343.

[33] H. Takahashi, P. J. Quinn, Hydration forces between phospholipid bilayers at subzero temperatures, Mol. Cryst. Liq. Cryst. 367 (2001) 427-434.

[34] G. I. King, C. R. Worthington, Analytic continuation as a method of phase

determination, *Phys. Lett.* 354 (1971) 259-260.

[35] J. F. Nagle, M. C. Wiener, Relation for lipid bilayers: Connection of electron density profiles to their structural quantities, *Biophys. J.* 55 (1989) 309-313.

[36] M. C. Wiener, R. M. Suter, J. F. Nagle, Structure of fully hydrated gel phase of DPPC, *Biophys. J.* 64 (1989) 315-325.

[37] M. J. Janiak, D.M. Small, G.G. Shipley, Nature of thermal pretransition of synthetic phospholipids: Dimyristoyl- and dipalmitoyllecithin, *Biochemistry* 15 (1976) 4575-4580.

[38] R. Koynova, B. G. Tenchov, S. Todinova, P.J. Quinn, Rapid reversible formation of a metastable subgel phase in saturated diacylphosphatidylcholines, *Biophys. J.* 68 (1995) 2370-2375.

[39] B. Tenchov, R. Koynova, M. Rappolt, G. Rapp, An ordered metastable phase in hydrated phosphatidylethanolamine: the Y-transition, *Biochim. Biophys. Acta* 1417 (1999) 183-90.

[40] S.C. Chen, J. M. Sturtevant, B. J. Gaffney, Scanning calorimetric evidence for sub-phase transition in phosphatidylcholine bilayers, *Proc. Natl. Acad. Sci. U. S. A.* 77 (1980) 5060-5063.

[41] M.J. Ruocco, G.G. Shipley, Characterization of the sub-transition of hydrated dipalmitoylphosphatidylcholine bilayers: X-ray diffraction study, *Biochim. Biophys. Acta* 684 (1982) 59-66.

[42] M.J. Ruocco, G.G. Shipley, Characterization of the sub-transition of hydrated dipalmitoylphosphatidylcholine bilayers: Kinetic, hydration and structural study,

Biochim. Biophys. Acta 691 (1982) 309-320.

[43] H.H. Fülde, Characterization of a third phase transition in multilamellar dipalmitoyl-lecithin liposomes, *Biochemistry* 20 (1981) 5707-5710.

[44] H. I. Petrache, S. Tristram-Nagle, J. F. Nagle, Fluid phase structure of EPC and DMPC bilayers, *Chem. Phys. Lipids* 95 (1998) 83-94.

[45] S. Tristram-Nagle, Y. Liu, J. Legleiter, J.F. Nagle, Structure of gel phase DMPC determined by X-ray diffraction, *Biophys. J.* 83 (2002) 3324-3335.

[46] R.N.A.H. Lewis, N. Mak, R. N. McElhaney, Differential scanning calorimetric study of the thermotropic phase behavior of model membranes composed of phosphatidylcholines containing linear saturated fatty acyl chains, *Biochemistry* 26 (1987) 61118-6126.

[47] S. Tristram-Nagle, Y. Isaacson, Y. Lyatskaya, Y. Liu, K. Brummond, J. Katsaras, J. F. Nagle, Polymorphism in Myristoylpalmitoylphosphatidylcholine, *Chem. Phys. Lipids* 100 (1999) 101-113.

[48] R.N.A.H. Lewis, R. N. McElhaney, Structures of the subgel phases of *n*-saturated diacyl phosphatidylcholine bilayers: FTIR spectroscopic studies of $^{13}\text{C}=\text{O}$ and ^2H labeled lipids, *Biophys. J.* 61 (1992) 63-77.

[49] J. Katsaras, V. A. Raghunathan, E.J. Dufourc, J. Dufourcq, Evidence for two-dimensional molecular lattice in subgel phase DPPC bilayers, *Biochemistry* 34 (1995) 4684-4688.

[50] C. P. Yang, J. F. Nagle, Phase transformations in lipids follow classical kinetics with small fractional dimensionalities, *Phys. Rev. A* 37 (1988) 3993-4000.

- [51] S. Tristram-Nagle, R. M. Suter, W.-J. Sun, J. F. Nagle, Kinetics of subgel formation in DPPC: X-ray diffraction proves nucleation-growth hypothesis. *Biochim. Biophys. Acta* 1192 (1994) 14-20.
- [52] C. M. Talbott, I. Vorobyov, D. Borchman, K.G. Taylor, D. B. Dupré, M.C. Yappert, Conformational studies of sphingolipids by NMR spectroscopy. II. Sphingomyelin, *Biochim. Biophys. Acta* 1467 (2000) 326-337.
- [53] E. Mombelli, R. Morris, W. Taylor, F. Fraternali, Hydrogen-bonding propensities of sphingomyelin in solution and in a bilayer assembly: A molecular dynamics study, *Biophys. J.* 84 (2003) 1507-1517.
- [54] S.W. Chiu, S. Vasudevan, E. Jakobsson, R.J. Mashl, H.L. Scott, Structure of sphingomyelin bilayers: A simulation study, *Biophys. J.* 85 (2003) 3624-3635.
- [55] R. H. Pearson, I. Pascher, The molecular structure of lecithin dihydrate, *Nature* 281 (1979) 499-501.

Figures

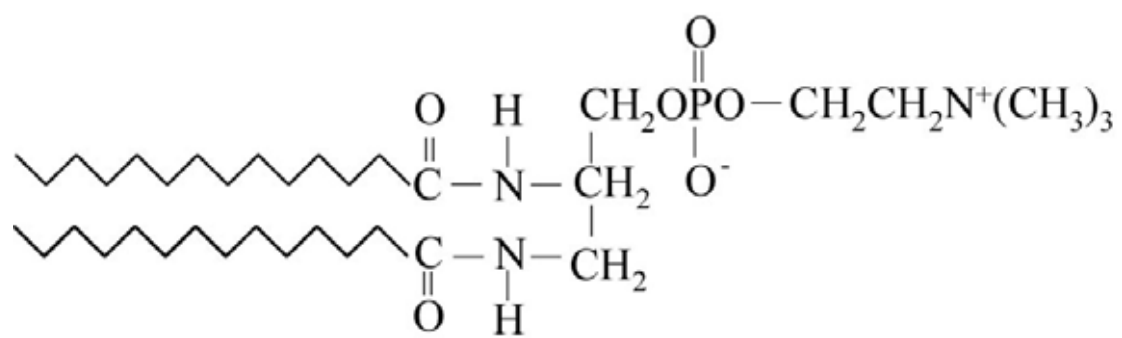


Figure 1.

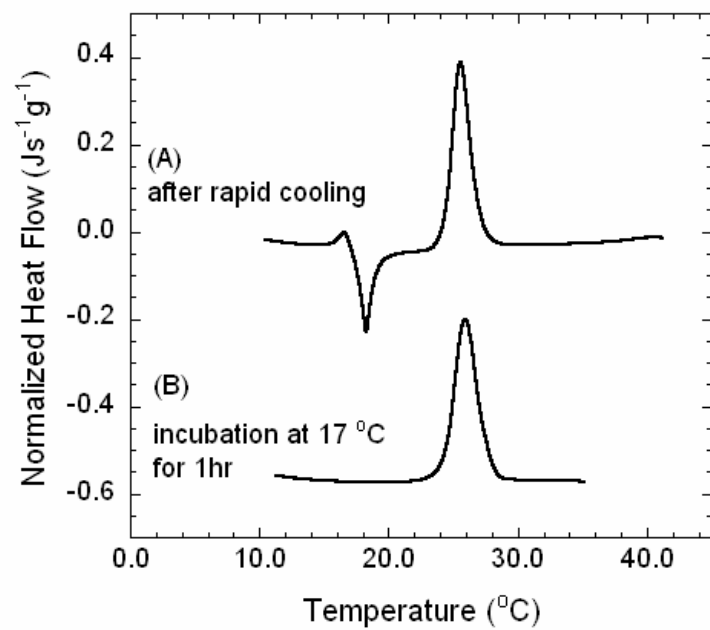


Figure 2

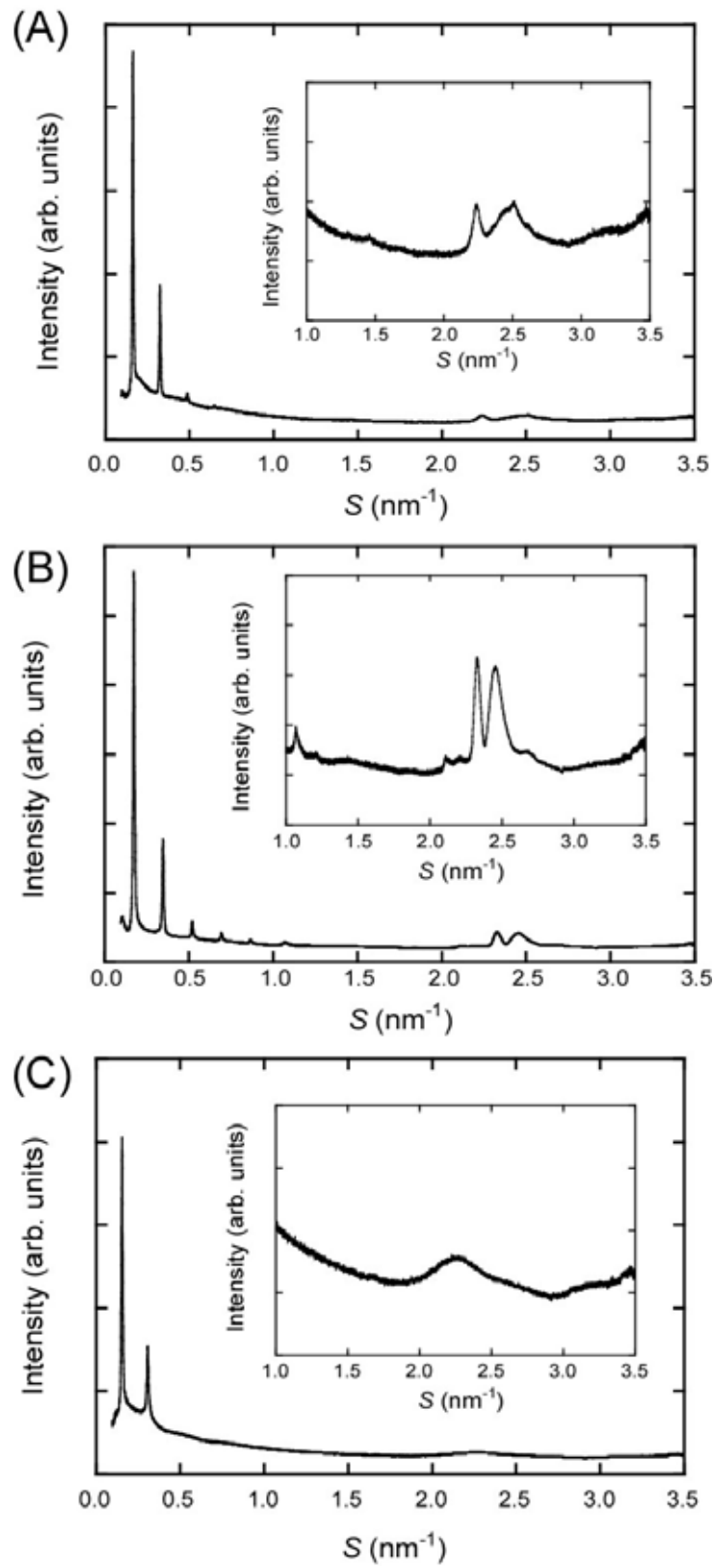


Figure 3

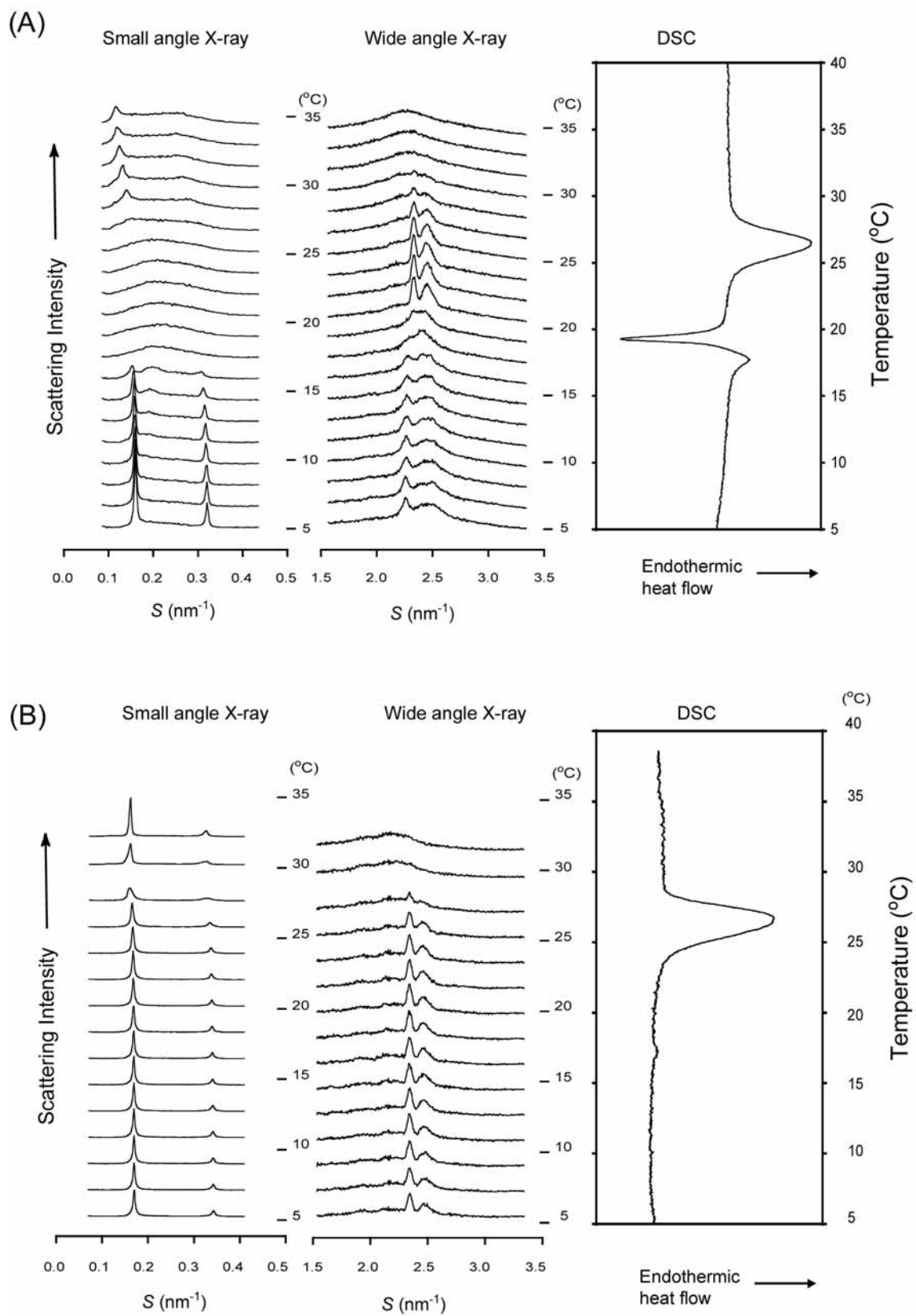


Figure 4

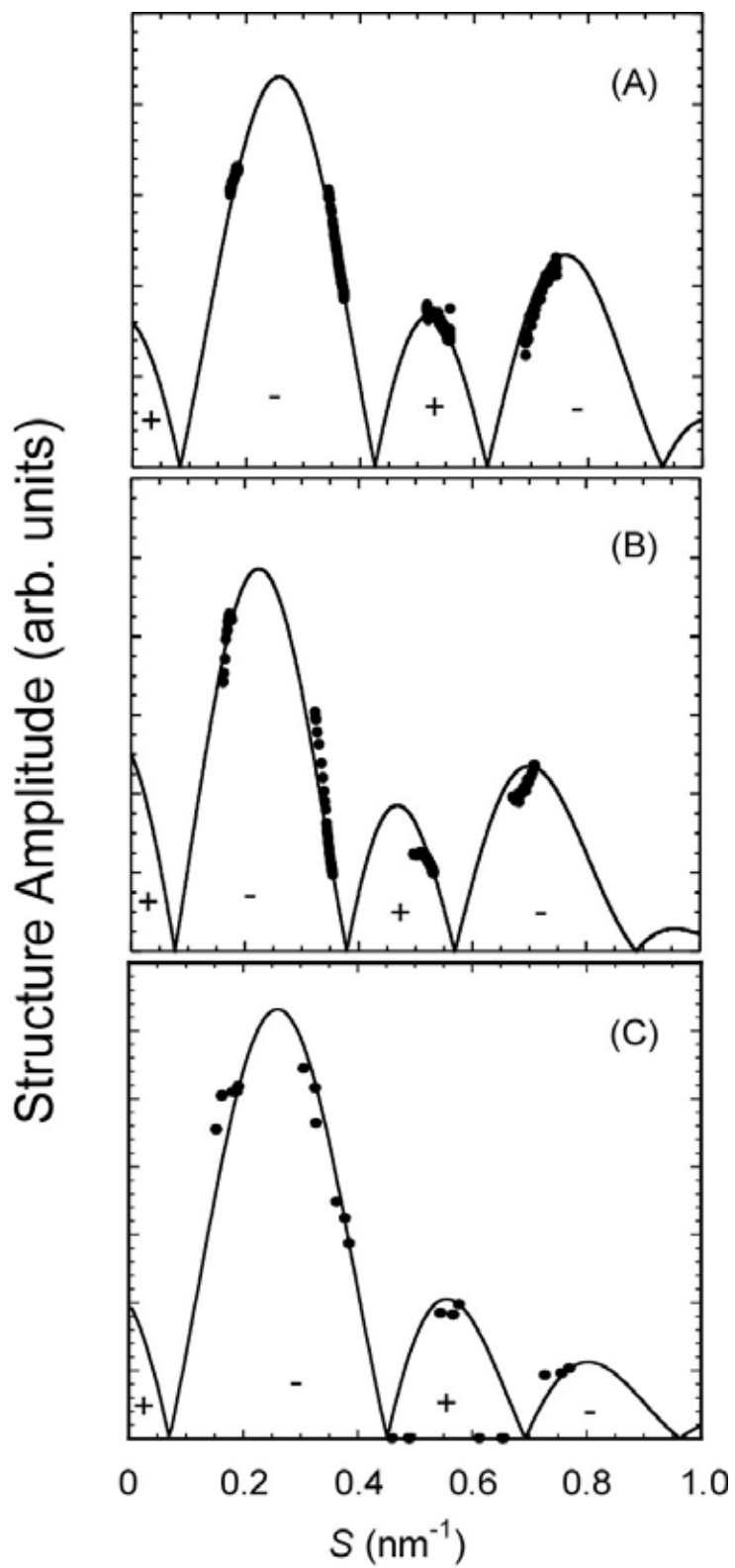


Figure 5

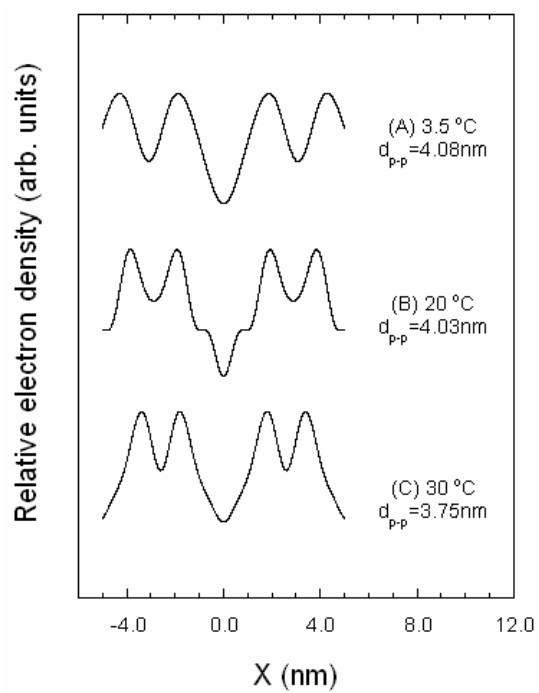


Figure 6

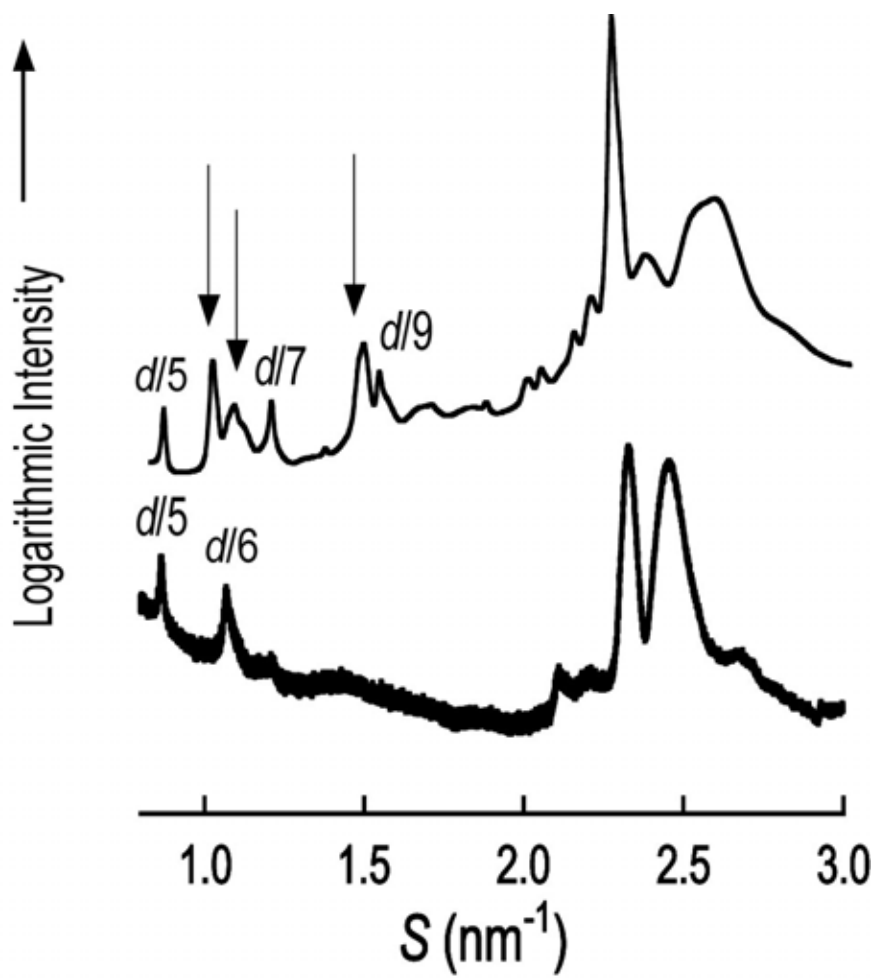


Figure 7